Intersubband Auger recombination and population inversion in quantum-well subbands

S. Borenstain and J. Katz*
Jet Propulsion Laboratory, California Institute of Technology, 4800 Oak Grove Drive, Pasadena, California 91109
(Received 5 August 1988)

The intersubband-Auger-recombination time of electrons under population-inversion conditions in a single quantum well is calculated by taking into account momentum- and energy-conservation rules, and by employing Fermi-Dirac statistics. The screened matrix element of the electron-electron interaction and the overlap integral are calculated for an infinitely deep quantum well. The results are in a good agreement with published experimental data. As a major nonradiative process, the Auger recombination is related to threshold current of infrared lasers based on intersubband transitions in quantum-well structures. The realization of these devices and other limitations to achieving population inversion are discussed. In view of the results, development of these lasers for emission wavelengths corresponding to energies below the LO-phonon energy seems feasible.

I. INTRODUCTION

Transition mechanisms between subband levels of confined carriers in semiconductor quantum-well structures (QWS) have attracted the attention of many investigators. Direct-absorption experiments between subbands with energy separation corresponding to wavelengths in the range of 4.4–10 μm (Refs. 1–5) demonstrated large values of dipole moment and oscillator strength. Recently, several authors[6,7] proposed QWS's where population inversion between the first and second subbands can be obtained, and hence stimulated emission in the infrared may be possible. Analysis by Yuh and Wang,[6] for a 10-μm transition wavelength, shows that an appreciable gain value of 1500 cm^{-1} may be achieved. The main advantages of these QWS's are the possibility of tuning the transition energy by changing the well width and depth and pumping by electrical-current injection. In particular, QWS's with wide wells may also provide a solution for realizing solid-state lasers operating at wavelengths in the far infrared (FIR), $\lambda \sim 100$ μm. In order to evaluate the threshold current of such a laser system and to find its possible operating-wavelength range, it is necessary to have a good knowledge of the fundamental, nonradiative processes which are involved in the intersubband-transition process. It is expected that, as is true with conventional narrow-band-gap-semiconductor lasers, the nonradiative-recombination rate in a degenerate quantum-well envelope-state transition[1] (QWEST) laser system may be dominated by Auger processes.[8]

Although the broad bandwidth of the measured absorption indicates a lifetime of less then 0.1 psec, direct, time-resolved experiments reveal much longer transition times. The broad bandwidth is due to the fast dephasing time, which is a result of the intrasubband e-e and e–acoustic-phonon scattering. In considering the magnitude of the current which is associated with the various transitions in a QWEST laser device, the intersubband transition time is the important factor. Intersubband relaxation time of the order of 10 psec, at 300 K, has been measured in a QWS with subband splitting corresponding to a wavelength of about 8.3 μm.[9] The experiment was performed by means of an infrared bleaching technique with picosecond time resolution. The relaxation time is relatively short due to the fast e–polar-LO-phonon interaction. Relaxation times have been measured also in a wide quantum well, with energy separation smaller than the energy of an optical phonon.[10] In this experiment, by using picosecond Raman spectroscopy, the total intersubband-transition time was found to be about 325 psec. Our results here show that the Auger relaxation mechanism is significant for energies below the LO phonon and therefore important in explaining this experiment.

Calculation of the intersubband Auger recombination in superlattices has been reported,[11] and there are also several theoretical investigations of Auger recombinations in QWS's (Refs. 12–16) all of which are expected to be applicable to a QWEST. However, with the exception of the early work by Chiu and Yariv,[12] none of them treated the problem of a degenerate electron system. Also, in more recent works by Smith *et al.*[15] and Basu,[16] it was recognized that simplified treatment of the confined envelope wave function in the matrix element can cause errors of more than 2 orders of magnitude. With the attention here on a single quantum well, we solve the problem of a degenerate electron gas and show that it is important to use Fermi-Dirac statistics in a situation where the Fermi energy of the electron gas in the upper subband is of the order of the subband splitting energy.

We also discuss other limitations that are intrinsically imposed on the degree of population inversion while realizing laser devices. Our results encourage the development of infrared lasers based on a QWEST for emission wavelengths corresponding to energies below the energy of the LO phonon.

II. MODEL

In our model, we assume that population inversion exists between the first and second subbands and consider a

single Auger process [Fig. 1(a)]. An electron in the second subband relaxes into an empty state in the first subband, while an electron of opposite spin is excited within the second subband from state 2 to state 2′. We also consider the impact-ionization process [Fig. 1(b)], which is the inverse of the Auger process. We neglect interaction with other subbands [Fig. 1(c)], an assumption that is justified in cases where the Fermi energy is smaller than the splitting energy. This, of course, sets an upper limit to the electron density in the upper subband in which our model is valid, above which relaxation times become shorter. Another possible process is described in Fig. 1(d), however, the process is not significant in situations where the lower subband is relatively empty. We also neglect the nonparabolicity of the conduction band and assume that the two subbands are characterized by the same effective mass. The parameters used in the calculations are those of GaAs: $\epsilon_r = 12$ and $m^* = 0.065 m_e$.

A. Matrix element

The matrix element of the screened electron-electron pair interaction is expressed as[17]

$$M = \int\int \Psi_{1'}^*(\mathbf{r}_1)\Psi_{2'}^*(\mathbf{r}_2) \times \left[\frac{e^2}{4\pi\epsilon_0\epsilon_r}\frac{\exp(-k_s|\mathbf{r}_1-\mathbf{r}_2|)}{|\mathbf{r}_1-\mathbf{r}_2|}\right] \times \Psi_1(\mathbf{r}_1)\Psi_2(\mathbf{r}_2)d\mathbf{r}_1 d\mathbf{r}_2 , \quad (1)$$

where k_s is the inverse of the screening length as discussed below. We take the wave functions to be those of an infinitely deep potential well, which is a good approximation for wide wells. In a quantum-well sample of area A and well width L_w, the wave functions are

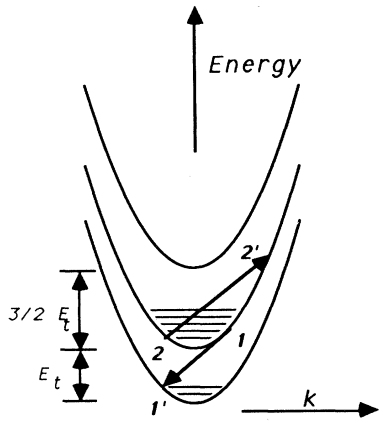

(a) Auger process with the two interacting electrons in the second subband.

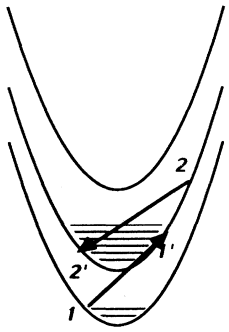

(b) Impact ionization process.

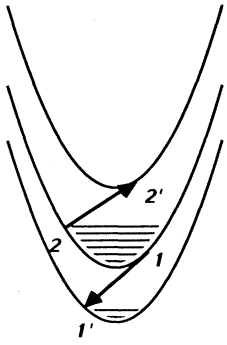

(c) Auger process with three subbands involved.

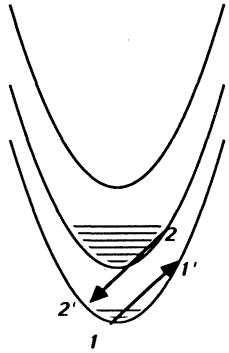

(d) Auger process with the two interacting electrons in the first and second subbands.

FIG. 1. Schematic description of the various electron-electron scattering processes which are involved in intersubband transition.

$$\Psi_i=\frac{1}{(AL_w)^{1/2}}[u_l^{(+)}(\mathbf{r})\exp(ik_{zl}z)+u_l^{(-)}(\mathbf{r})\exp(-ik_{zl}z)]e^{-i\mathbf{k}_i\cdot\boldsymbol{\rho}} . \quad (2)$$

Outside the well, $\Psi_i(\mathbf{r})=0$. In subband l, $k_{zl}=l\pi/L_w$, and $u_l^{(+,-)}$ are the periodic parts of the Bloch functions. $\mathbf{k}$ is the two-dimensional (2D) wave vector in the plane of the well and $\boldsymbol{\rho}$ is the 2D position vector. In our calculation of the matrix element, we make use the results of Smith *et al.*[15] and modify them to include screening:

$$M=\frac{e^2}{4\pi\epsilon_0\epsilon_r}\frac{2\pi}{L_w^2A^2}\delta(\mathbf{k}_1-\mathbf{k}_{1'}+\mathbf{k}_2-\mathbf{k}_{2'})\times\int_{-\infty}^{+\infty}\frac{\{1',1,q_z\}\{2',2,-q_z\}}{|\mathbf{k}_{2'}-\mathbf{k}_2|^2+q_z^2+k_s^2}dq_z . \quad (3)$$

The terms in the curly brackets denote the overlap integral between the 2D subband envelope functions and the z component of the Fourier transform of the Coulomb interaction:

$$\{n,m,q_z\}=H(k_{zn}-k_{zm}+q_z)+H(-k_{zn}+k_{zm}+q_z)+H(-k_{zn}-k_{zm}+q_z)+H(k_{zn}+k_{zm}+q_z) , \quad (4)$$

where $H(p)=L_w\sin(pL_w/2)/(pL_w/2)$. A standard method of dealing with the overlap integral is through the momentum-conversation approximation (MCA),[18] leaving only selection rules for the interaction. However, the intersubband interaction discussed here is one of the cases where the MCA does not hold. Under the MCA, intersubband interaction is prohibited and thus we have to perform a more exact calculation of these overlap integrals. The multiplication of the overlap integral in (3) gives

$$\{1',1,q_z\}\{2',2,-q_z\}=2\sin(q_zL_w)\left[\frac{2}{q_zL_w}+\frac{1}{4\pi+q_zL_w}-\frac{1}{4\pi-q_zL_w}\right]\times\left[\frac{1}{\pi+q_zL_w}+\frac{1}{\pi-q_zL_w}-\frac{1}{3\pi-q_zL_w}-\frac{2}{3\pi+q_zL_w}\right] \quad (5)$$

and is plotted in Fig. 2. From this result it is seen that screening must be introduced, otherwise (i.e., if $k_s=0$), the matrix element in Eq. (3) will diverge at $\mathbf{k}_2-\mathbf{k}_2'=\mathbf{0}$.

The inverse of the screening length is given by[19]

$$k_s^{-1}=\frac{e^2}{\epsilon_0\epsilon_r k_BT}\frac{2}{L_w(2\pi)^2}\int f(k)[1-f(k)]d\mathbf{k}^2 , \quad (6a)$$

where k_B is the Boltzmann constant, T is the temperature, and f is the Fermi-Dirac distribution. In the calculations here we use two approximations of (6a). For low electron density and high temperature, we use the Debye screening:

$$k_s^2=\frac{e^2}{k_BT4\pi\epsilon_0\epsilon_r}\left[\frac{n}{L_w}\right] . \quad (6b)$$

And for the degenerate case, we use the approximation

$$k_s^2=\frac{m^*e^2}{4\pi\epsilon_0\epsilon_r}\left[\frac{n}{L_w}\right]^{1/3} . \quad (6c)$$

For a given temperature and 2D-electron density n, we take the smaller screening length of the two.

We note that in contrast to calculations of band-to-band Auger transition, knowledge of the periodic part of the wave function is not essential, since the initial and final Bloch functions are of the conduction band, and therefore identical, the intergration over that part of the matrix element yields unity.

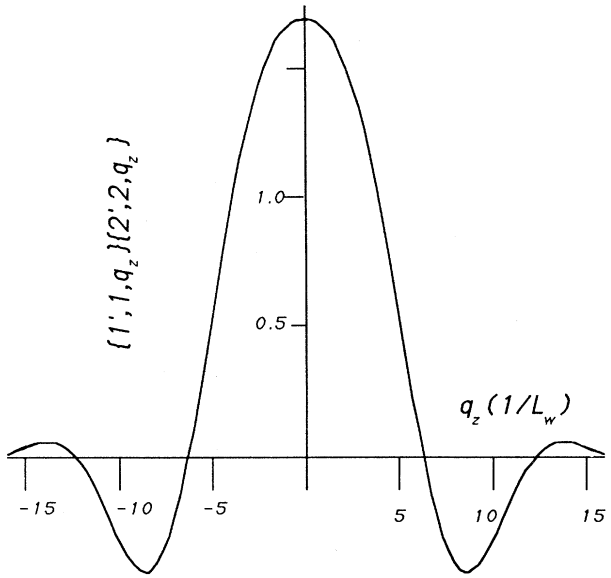

FIG. 2. The overlap integral (dimensionless), as a function of the z component of the Fourier-transformed Coulomb interaction [Eq. (5)].

B. Transition rate

The net rate of the Auger transition (i.e., compensated by the impact-ionization process) can be written as

$$R=\frac{2\pi}{\hbar}\left[\frac{A}{4\pi^2}\right]^4\times\int|M|^2P_{11'22'}\delta(\mathbf{k}_1-\mathbf{k}_{1'}+\mathbf{k}_2-\mathbf{k}_{2'})\times\delta(E_f-E_i)d^2\mathbf{k}_1d^2\mathbf{k}_2d^2\mathbf{k}_{1'}d^2\mathbf{k}_{2'} , \quad (7)$$

where $P_{11'22'}$ is the probability factor:

$$P_{11'22'}=f_1f_2(1-f_{1'})(1-f_{2'}) -f_{1'}f_{2'}(1-f_1)(1-f_2) . \quad (8)$$

f_i is the Fermi-Dirac distribution function in state i, $f_i=\{1+\exp[(E_i-F_l)/k_BT]\}^{-1}$, and F_l is the quasi-Fermi-energy in subband l and is related to the 2D-electron density n_l by $F_l=E_l+k_BT\ln[\exp(n_1/Dk_BT)-1]$, where D is the 2D-electron sheet density of states $D=m^*/\pi\hbar^2$. In the approximation where the quantum well is infinetely deep, the splitting energy is related to the well width by $E_t=3/2m^*(\pi\hbar/L_w)^2$. The two interacting electrons in the initial states have 2D wave vectors $\mathbf{k}_1$, $\mathbf{k}_2$, and kinetic energies $E_{1,2}=E_t+\hbar^2k_{1,2}^2/2m^*$. The constraints set by energy and momentum conservation determine the final energy and 2D $\mathbf{k}$ vectors:

$$k_{2'}=\tfrac{1}{2}\{k_2\cos\phi_2-k_1\cos\phi_1 +[(k_1\cos\phi_1-k_2\cos\phi_2)^2 +2k_t^2+4k_1k_2\cos(\phi_1-\phi_2)]^{1/2}\} , \quad (9)$$

$$k_{1'}^2=k_{2'}^2+k_2^2+k_1^2-2k_1k_2\cos(\phi_1-\phi_2) -2k_{2'}k_2\cos\phi_2+2k_1k_{2'}\cos\phi_1 , \quad (10)$$

where $k_t=(2m^*E_t/\hbar^2)^{1/2}$ and ϕ_1,ϕ_2 are the angles of $\mathbf{k}_1,\mathbf{k}_2$, respectively, relative to $\mathbf{k}_{2'}$. By transforming the integral in (7) into the energy representation, one obtains

$$R=\frac{2\pi}{\hbar}(\pi D)^3 2\pi\left[\frac{A}{4\pi^2}\right]^4 \times\int_0^\infty dE_1\int_0^\infty dE_2\int_0^{2\pi}d\phi_1\int_0^{2\pi}d\phi_2(|M|^2P_{11'22'}) , \quad (11)$$

and the Auger-recombination time is defined as

$$\tau_{Au}=\frac{n_2-n_0}{R}\sim\frac{n_2}{R} , \quad (12)$$

where n_0 is the equilibrium value of the density.

In the framework of *Fermi's golden rule,* Eq. (11), combined with the conservation rules (9) and (10), is exact and is also relatively easy to calculate numerically.

III. RESULTS AND DISCUSSION

A. Auger-recombination rate

We discuss first the solution of (11) with constant matrix elements, in order to find the dependence of the probability factor on the transition energy. Referring to inset (a) of Fig. 3, it is seen that all possible final states (2′) of the interacting electrons are occupied since energy conservation forces the energy of states 2′ to be $E_2+E_t-E_1-E_{1'}\sim E_t$ which is below the Fermi energy. Therefore, unless the initial energy E_2 is about the Fermi energy, Auger transition is not allowed and $P_{11'22'}\sim0$. On the other hand [inset (b) of Fig. 3], in a system where the Fermi energy is the same but with much higher splitting energy, interaction is possible for electrons with any initial energy E_2. It is concluded then that in the latter case the integral over E_2 in (11) will yield a higher total Auger-transition rate and it also explains the trend of the recombination time shown in Fig. 3. This result is in contradistinction with that obtained while solving the Auger-transition rate with nondegenerate statistics. In that approach, a probability factor for the most probable transition (where the initial states of the interaction are near Fermi energy) replaces the integral over all partially probable transitions.[20] It is thus obvious that when the Fermi energy is of the order of the splitting energy, this approximation is no longer valid.

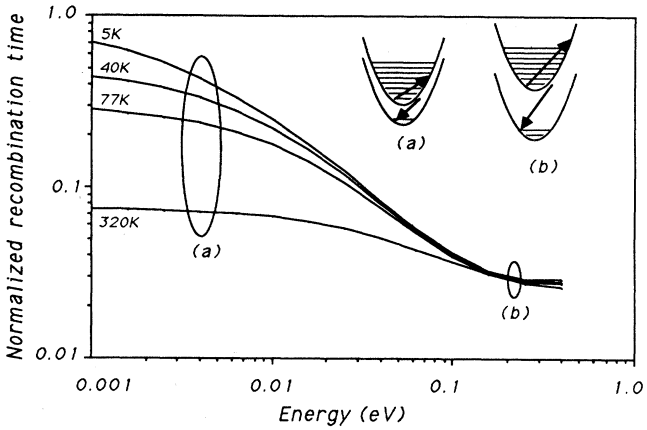

FIG. 3. Normalized intersubband Auger recombination time as a function of the subband splitting energy. The matrix element in the calculations is taken as a constant and $n_2=10^{12}$ cm^{-2}, $n_1=10^{10}$ cm^{-2}. These results demonstrate the significant dependence of the transition rate on the probability factor $P_{11'22'}$. (a) Splitting energy smaller than the quasi-Fermi-energy of the second subband. Depicted Auger transition is virtually prohibited at low temperatures (i.e., $P_{11'22'}$ is negligible), resulting in long Auger-recombination time. (b) Splitting energy larger than the quasi-Fermi-energy of the second subband. Depicted transition is allowed (i.e., $P_{11'22'}$ is large), resulting in the shortening of Auger-recombination time as compared to (a).

Calculations results of the Auger-recombination time as a function of the splitting energy, for two different temperatures and electron densities, are shown in Fig. 4. From these results it is seen that the Auger-recombination time is not a sensitive function of temperature, and that at low splitting energies it also becomes less sensitive to the injected electron density. However, we note that Eq. (11) yields accurate results for a limited range of the electron-density value. For example, for a 10^{12} cm^{-2} electron density and $D=2.72\times10^{13}$ eV^{-1}cm^{-2}, the Fermi energy is ~37 meV, and, therefore, below $E_t\sim60$ meV processes of the type described in Fig. 1(c) will also take place, and thus the actual recombination time will become shorter. For 10^{11} cm^{-2} the model is accurate down to $E_t\sim6$ meV.

We now compare the calculation results to the relevant experiment, where E_t is sufficiently small so that there is no LO-phonon-assisted recombination.[10] The reported

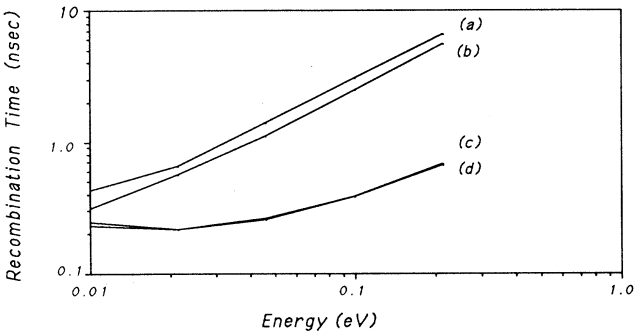

FIG. 4. Intersubband Auger-recombination time as a function of the subband splitting energy. Calculation includes detailed calculation of a the matrix element. The various parameters of each curve are (a) $n_2=10^{11}$ cm^{-2}, $T=5$ K; (b) $n_2=10^{11}$ cm^{-2}, $T=40$ K; (c) $n_2=10^{12}$ cm^{-2}, $T=5$ K; (d) $n_2=10^{12}$ cm^{-2}, $T=40$ K. In all the calculations n_1 is taken as 10^{10} cm^{-2}.

experimental parameters are for $Ga_{0.7}Al_{0.3}As/GaAs$ multiple-quantum-well structure, with a well width of 215 Å and splitting energy $E_t=26.8$ meV. The reported electron density is 4×10^{11} cm^{-2}, corresponding to a Fermi energy of 15 meV. The experimental result of 325 psec is composed of three components:

$$\tau_{21}^{-1}=\tau_r^{-1}+\tau_{\mathrm{Au}}^{-1}+\tau_p^{-1}\ , \tag{13}$$

where τ_r is the radiative lifetime of the second subband and τ_p is the lifetime component associated with the acoustic-phonon-assisted recombination. The experimental parameters are within the scope of our model, and under similar parameters we obtain an (Fig. 4) Auger-recombination time of $\sim$600 psec. As for τ_p, calculation of *intra*subband electron–acoustic-phonon-scattering time in $Ga_{1-x}Al_xAs$ heterostructures gives about 400 psec.[21] *Inter*subband scattering, however, involves multiphonon scattering as well as scattering of phonons with large momentum values. This makes the phonon-assisted intersubband-relaxation time much longer. The radiative-recombination time consists of interband and intersubband components. The intersubband component is given by

$$\tau_r^{-1}=\frac{\bar{n}e^2 2\pi}{m_0\epsilon_0\lambda^2 c}f_{ij}\ . \tag{14}$$

With the GaAs intersubband-oscillator strength of $f_{12}\sim15$ (Ref. 1) and refraction index $\bar{n}\sim3.3$ at $\lambda=46.3$ μm, the intersubband recombination time of 0.7 μsec is too long to be important. In a photoexcited situation, as is the case in the discussed experiment, the interband radiation is much faster, but is estimated to be longer than 750 psec.[10] All these recombination time values can adequately explain the experimental result.

B. Stimulated emission

With the model structure shown schematically in Fig. 5, we discuss the realization of population inversion in

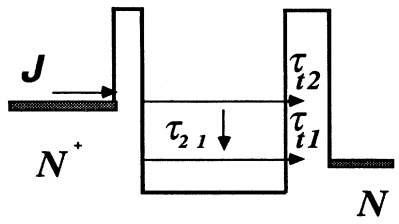

FIG. 5. Schematic structure depicting the basic principles of creating population inversion in quantum-well subbands by current injection.

QWS's. A feature common to all the devices proposed is current injection by resonant tunneling from one side of the active layer to the upper subband, and resonant tunneling from the lower subband to the other side of the active layer. For a population inversion to take place, it is ideally required that there will be tunneling only in a narrow energy band, centered in each subband energy. In a realistic situation, however, leaky nonresonant tunneling of electrons from the upper level to the adjacent layer also exists. This effect can be described by the following set of simplified rate equations:

$$\frac{dn_2}{dt}=\frac{J}{e}-\frac{n_2}{\tau_{21}}-\frac{n_2}{\tau_{t2}}\ , \tag{15a}$$

$$\frac{dn_1}{dt}=\frac{n_2}{\tau_{21}}-\frac{n_1}{\tau_{t1}}\ , \tag{15b}$$

where J is the current density, τ_{t1} is the time required for an electron to tunnel from the lower subband to the adjacent layer, and τ_{t2} is the leaky, nonresonant tunneling time. In a steady-state condition the population inversion is

$$n_2-n_1=\frac{J}{e}\left[\frac{\tau_{t2}}{\tau_{t2}+\tau_{21}}\right](\tau_{21}-\tau_{t1})\ . \tag{16}$$

In a situation where $\tau_{21}\gg\tau_{t2}$ and also $\tau_{21}\gg\tau_{t1}$, we obtain

$$n_2-n_1\sim\frac{J\tau_{t2}}{e}\ . \tag{17}$$

From this analysis we see that the leaky tunneling may set a severe limitation on the obtainable population inversion. Leaky tunneling is mainly a result of phonon-assisted tunneling or tunneling assisted by inelastic scattering from potential fluctuations that are present, e.g., because of rough interfaces and impurities. Leaky tunneling may be reduced by low-temperature operation and good control of the growth conditions. If we assume that leaky-tunneling time is given by the peak-to-valley ratio times the resonant tunneling time of a resonant tunneling diode, we obtain $\tau_{t2}>300$ psec.[22] Under these conditions, for a current density of $J=1000$ A/cm^2, population inversion of 10^{12} cm^{-2} may be achieved. Although the quantum efficiency defined by $\eta=\tau_{\mathrm{nr}}/(\tau_{\mathrm{nr}}+\tau_r)$, where τ_{nr} includes contributions of all nonradiative pro-

cesses, i.e $\tau_{nr}^{-1}=\tau_{t2}^{-1}+\tau_{Au}^{-1}+\tau_p^{-1}$, at $\lambda\sim 100$ μm is low, $\eta\sim 10^{-4}$, complete evaluation of threshold current for lasing has to take into account the balance of gain to absorption in any particular wavelength. Our calculations for this system[23] give gain values in excess of the absorption, with reasonable current densities. Once the current is above threshold the quantum efficiency increases abruptly due to the short stimulated emission recombination time.

IV. CONCLUSIONS

We have calculated the Auger-recombination time of electrons under population inversion in quantum-well subbands as a function of the splitting energy. We have taken into account Fermi-Dirac statistics and have shown the importance of this approach in cases where the splitting energy is comparable to the Fermi energy and have found that Auger processes are long enough to allow a high degree of population inversion. We have also shown that leaky, nonresonant tunneling is the dominant competing process to radiative transitions in systems driven by injected current. However, high gain values of these transitions makes laser operation possible even in energies below the LO-phonon energy (i.e., $\lambda\sim 100$ μm). We expect the devices to be sensitive to temperature mainly because of the leaky currents, where phonon-assisted tunneling plays a major part.

ACKNOWLEDGMENTS

The authors wish to thank R. W. Terhune for useful discussions. One of the authors (S.B.) thanks the National Research Council for their support. The work described in this paper was carried out as part of the Center for Space Microelectronics Technology of the Jet Propulsion Laboratory, and was sponsored by the Strategic Defense Initiative Organization Innovative Science and Technology Center through an agreement with the National Aeronautics and Space Administration.

---

*Present address: Symbol Technologies, Inc., 116 Wilbur Place, Bohemia, NY 11716-3300.

[1]L. C. West and S. J. Eglash, Appl. Phys. Lett. **46**, 1153 (1985).
[2]B. F. Levine, R. J. Mallik, J. Walker, K. K. Cohi, C. G. Bethea, D. A. Kleinman, and J. M. Vandenberg, Appl. Phys. Lett. **50**, 273 (1987).
[3]M. Nakayama, H. Kuwahar, H. Kato, and K. Kubato, Appl Phys. Lett. **51**, 1741 (1987).
[4]B. F. Levine, R. J. Malik, J. Walker, K. K. Choi, C. G. Bethea, K. A. Kleinman, and J. M. Vandenberg, Appl. Phys. Lett. **50**, 273 (1987).
[5]B. F. Levine, A. Y. Cho, J. Walker, R. J. Mallik, D. A. Kleinman, and D. L. Sivco, Appl. Phys. Lett. **52**, 1481 (1988).
[6]P. F. Yuh and K. L. Wang, Appl. Phys. Lett. **51**, 1404 (1987).
[7]H. C. Liu, J. Appl. Phys. **63**, 2856 (1988).
[8]For a review on Auger processes in bulk materials, see P. T. Landsberg, Solid State Electron. **30**, 1107 (1987).
[9]A. Seilmeir, H. J. Hubner, G. Abstreiter, G. Weinmann, and W. Schlapp, Phys. Rev. Lett. **59**, 1345 (1987).
[10]D. Y. Oberly, D. R. Wake, M. V. Klein, J. Klem, T. Henderson, and H. Morkoç, Phys. Rev. Lett. **59**, 696 (1987).
[11]P. F. Yuh and K. L. Wang Phys. Rev. B **37**, 1328 (1988).
[12]L. C. Chiu and A. Yariv, IEEE J. Quantum Electron. **QE-18**, 1406 (1982).
[13]N. K. Dutta, J. Appl. Phys. **54**, 1236 (1983).
[14]A. Sagimura, IEEE J. Quantum Electron. **QE-19**, 932 (1983).
[15]C. Smith, R. A. Abram, and M. G. Burt, J. Phys. C **16**, L171 (1983).
[16]P. K. Basu, J. Appl. Phys. **56**, 3334 (1984).
[17]B. K. Ridely, *Quantum Processes in Semiconductors* (Clarendon, Oxford, 1982), p. 268.
[18]B. K. Ridley, J. Phys. C **15**, 5899 (1982).
[19]H. C. Casey, Jr. and M. B. Panish *Heterostructure Lasers* (Academic, New York, 1978), Pt. A, p. 135. See also Ref. 12.
[20]The basis for the approximations used by most nondegenerate calculations are based on the paper by P. T. Landsberg, Solid State Commun. **10**, 479 (1972).
[21]M. Artaki and K. Hess, Phys. Rev. B **37**, 2933 (1988).
[22]A discussion on resonant tunneling time can be found, e.g. in T. C. L. G. Sollner, E. R. Brown, W. D. Goodhue, and H. Q. Lei, Appl. Phys. Lett. **50**, 332 (1987). A peak-to-valley ratio of 63 at 77 K was reported by Tom P. E. Broekaert, Wai Lee, and Clifton G. Fonstad, Appl. Phys. Lett., **53**, 1545 (1988).
[23]S. Borenstain and J. Katz (unpublished).